



Fouling mechanisms and primary foulant constituents in reverse osmosis membrane reclamation of a petrochemical secondary effluent

Haigang Li¹, Ping Yu*, Yunbai Luo

College of Chemistry and Molecular Sciences, Wuhan University, Wuhan 430072, P.R. China, Tel. +86 27 68752511; Fax: +86 27 68752511; email: yuping@whu.edu.cn

Received 12 October 2013; Accepted 26 March 2014

ABSTRACT

In this study, fouling in the system of reverse osmosis (RO) fed with ultrafiltration prefiltered petrochemical secondary effluent was studied by using a laboratory-scale RO setup. With the micro-analysis of the fouling layer, the residual organic foulants were found to be the primarily responsible elements for the evolution of irreversible fouling. After characterization of the dissolved organic matter in the wastewater with gas chromatograph-mass spectrometer, it had been identified that aromatic compounds and hydrocarbon compounds were the major chemicals. With the help of Fourier transformed infrared spectra, the aromatics were detected to be the predominant organic foulants found on the membrane surface. According to results of electron-dispersive X-ray microanalysis spectrometry, metal cations such as Fe³⁺ and Mg²⁺ also contributed to irreversible fouling to some extent. This study identified that reducing adsorption of the organics on the membrane surface is a more effective way or method to control membrane fouling in the reclamation of the secondary effluent.

Keywords: Membrane fouling; Petrochemical secondary effluent; Irreversible fouling; GC-MS; FTIR

1. Introduction

An extremely important issue in twenty-first century is access to secure, sustainable sources of freshwater. Capturing water directly from industrial wastewater and treating it have been receiving much attention [1]. Although reverse osmosis (RO) is considered as the current state-of-the-art water recycling technology, membrane fouling is still the most important obstacle to the efficient application [2] particu-

larly when fouling leads to flux decline which cleaning cannot restore [3]. Pretreatment techniques, including active sludge, chemical oxidation, dual-media filtration, microfiltration, and ultrafiltration (UF) can potentially remove foulants prior to RO filtration. However, adsorption of the residual organic matters on the RO membrane surface leads to flux decline. Adsorption of the organics onto the membrane surface leads to a reduction of the pure water permeability [4]. In addition, as the organics accumulating on the membrane surface, it acts as nucleation

*Corresponding author.

¹Current address: Key Laboratory of Green Process and Engineering, Institute of Process Engineering, Chinese Academy of Sciences, P.R. China.

sites for sparingly soluble salts or entrapping particulates which further aggravates membrane fouling [5]. Furthermore, the organic foulants will chemically degrade membrane materials [6]. As a result, water-permeating flux decreases and in most cases, low-molecular-weight contaminants removal and salt rejection decrease seriously [3].

Flux decline are caused by concentration polarization and membrane fouling [7,8]. Concentration polarization causes flux decline in two possible tracks. Firstly, concentration polarization boundary layer induces the increase of the hydraulic resistance and osmosis pressure. Secondly, the elevated concentration of solutes near the membrane surface more or less affects membrane fouling. Membrane fouling is caused by the foulants in the wastewater that adhere to the membrane surface. Normally, foulants can be classified into four categories: the inorganics, the organics, particulates, and the microbiological organisms [9]. Membrane fouling can be divided into reversible and irreversible fouling depending on the efficiency of the chemical cleaning. For reversible fouling, the flux can be restored through controlling the operating conditions and proper membrane cleaning, while in the irreversible fouling case, the flux cannot be recovered by even aggressive cleaning.

The petrochemical industry consumes significant quantities of freshwater, and consequently, corresponding amounts of wastewater are generated and discharged. Hence, the reclamation of the petrochemical secondary effluent has become an increasing concern [10,11]. The dual membrane (UF-RO) process is capable of reclaiming the industrial secondary effluent [12]. In the dual membrane process, the effluent fed to the RO first passes through the UF. Reclaimed water can be used for cooling, process, and fire extinction in the factory. To date, however, little systematic studies have been done to evaluate membrane fouling caused by a petrochemical secondary effluent. Most of the fouling studies are conducted with synthetic wastewater [13–15].

Therefore, the purpose of this work was to identify primary foulants causing irreversible fouling on the membrane. The membrane was cleaned by a chemical agent. Based on the cleaning, irreversible fouling was mainly governed by organic fouling rather than by inorganic-scale fouling. Combining the characteristics of the wastewater and the analysis of the fouling layer on the membrane, we found that the organic fouling was mainly caused by the aromatics remaining on the membrane surface. The aromatics were conjectured to be phenol, methylphenol, benzeneacetic acid, dibutyl phthalate, and xylenol.

2. Materials and methods

2.1. Wastewater

The wastewater used in this experiment was UF pre-filtered secondary effluent collected from a local petrochemical plant. The treatment of the original wastewater was performed via a nitrifying-activated sludge process. The effluent further went through a biological aerated filter followed by 0.010 m quartz sand filter. The effluent from the sand filter passed through the submerged inside-out polyvinylidene fluoride UF equipped with 0.020 μm laminated filter. To control membrane biofouling, sodium hypochlorite was added to the UF feed water. The disinfected UF filtrate taken from the UF filtrate tank was collected in 25 L plastic casks. The concentration of the active chlorine was adjusted by Na_2SO_3 . The adjusted water samples were directly utilized as RO feed water and stored at 4°C in darkness. The charge density (carboxylic and phenolic acidity) of the wastewater was determined by potentiometric titration [16]. The concentration of anion and cation were analyzed using an ion chromatography (883 Basic, Metrohm, Switzerland). The organic composition of the wastewater was analyzed by using gas chromatograph-mass spectrometer (GC-MS) (6890N-5973N, Agilent, USA).

2.2. RO membrane

An aromatic polyamide thin-film composite membrane CPA2 from Nitto Denko Co., Ltd, (Osaka, Japan) was used in this study. The membrane element was tested at the standard test condition of 15.5 bar (225 psi) pressure and 25°C temperature with a 25.65 mM (1,500 mg L^{-1}) NaCl feed solution. Average salt rejection and water recovery were 99.7 and 15%, respectively. The air–water contact angle of the CPA2 membrane is $35 \pm 1.3^\circ$. Zeta-potential was measured to characterize the charge property of the membrane because electrokinetic property was an important factor in pressure-driven membrane water filtration process [17]. The zeta-potentials for the membrane CPA2 at pH 3.0, 7.0, and 10.0 were 22.76, -50.93 , and -51.05 mV, respectively. The membrane coupons were stored in deionized (DI) water at 4°C with water replaced regularly prior to experiments.

2.3. Fouling and cleaning experiments

A laboratory-scale crossflow test unit was used to perform fouling and cleaning experiments. The unit consists of a round membrane cell, high-pressure pump, electromagnetic mixer, feed tank, and

temperature control system. More details can be found from our previous work [18]. The bulk solution was held in a 5.0 L tank and fed to the membrane cell by a high pressure pump (Jingqiao, JW-C, Jingxin Pump Manufacturing Co., Ltd, Huai'an, China). The effective surface area of the membrane in contact with feed solution was 46.5 cm². Both permeate and retentate were not recirculated into the feed reservoir.

A new membrane specimen was used for each crossflow experiment. The membrane was first compacted with DI water (foulant-free) at 20.7 bar (300 psi) until the permeate flux stabilized. Temperature and feed pH were adjusted and maintained at the required values. Unless otherwise specified the initial flux and crossflow velocity were 21.0 μm s⁻¹ and 9.8 × 10⁻² m s⁻¹, respectively. After the feed tank was filled by the effluent instead of the DI water, fouling experiments were initiated. The permeate flux was continuously monitored until the flux was approximately stable.

At the end of fouling experiments, the pure water flux was measured. Then the fouled membrane was cleaned by the chemical cleaning solution. Cleaning was performed for 1.0 h at the normal atmosphere, 25°C, and crossflow velocity 30.1 × 10⁻² m s⁻¹. The solution was continuously circulated from the feed tank to the membrane in the cell. At the end of cleaning, the chemical cleaning solution in the tank was disposed. The tank and the membrane cell were rinsed with DI water to flush out the residual solution. Finally, the pure water flux was measured to determine the extent of irreversible flux decline. At this stage, the operating conditions of the pure water permeate flux determination were identical to those applied during fouling experiments. The experiment was performed three times.

2.4. Analyses

GC-MS: Samples for GC-MS analysis were prepared by micro solid-phase extraction. A HP-5MS capillary column (30 m length × 0.25 mm ID × 0.25 μm film thicknesses) was employed. Analysis was performed in a temperature-programmed mode with an initial temperature of 35°C held for 8 min, followed by a ramp of 3°C min⁻¹ to 200°C. The ion-source temperature was 250°C, and the carrier gas was high-purity helium gas. The spectra were searched in National Institute of Standards and Technology (NIST) library. Combining with the characteristics of the petrochemical wastewater, we confirmed the constituents of the wastewater.

EDX: The elemental composition of the membranes was analyzed by an electron-dispersive X-ray

microanalysis (EDX) spectrometry (FEI Quanta 200, Holland). The membrane samples were vacuum dried at ambient temperature before analysis.

FTIR: The attenuated total reflection-Fourier transform infrared spectroscopy analyses were performed by using the Nicolet AVATAR 360 FT-IR Spectrophotometer. The spectra measurements were performed at 10 different locations, with each spectrum averaged from 64 scans. FTIR spectrum of the stripped foulant was also collected in the transmission mode to confirm the organic composition. The fouled membrane was cleaned by the chemical agent and then vacuum dried at ambient temperature. The foulant was stripped off the cleaned membrane by a razor carefully.

2.5. Calculations

Membrane permeate flux can be estimated as following,

$$J = \frac{\Delta P}{\mu R} = \frac{P - \Delta\pi}{\mu(R_m + R_f)} \quad (1)$$

where P is the operation pressure, $\Delta\pi$ is osmotic pressure of solution, μ is the water viscosity, R is the total membrane resistance, R_m is the intrinsic membrane resistance, R_f is the fouling resistance, and ($\Delta P = P - \sigma\Delta\pi$) is represented as the transmembrane pressure (TMP).

The relative flux (RF) and flux recovery (FR) were defined by Eqs. (2) and (3), respectively,

$$\text{RF} (\%) = \frac{J_b}{J_w} \times 100 \quad (2)$$

$$\text{FR} (\%) = \frac{J_{fw}}{J_w} \times 100 \quad (3)$$

where J_w , J_b , and J_{fw} are the pure water flux of virgin membrane, wastewater flux, and pure water flux of fouled membrane, respectively.

The irreversible recovery (IR) was defined as Eq. (4),

$$\text{IR} (\%) = 100 - \frac{J_{cw}}{J_w} \times 100 \quad (4)$$

where J_{cw} is the pure water flux of the chemical cleaning membrane.

In this case, 100-RF corresponds to the total flux decline caused by concentration polarization and fouling. IR corresponds to the irreversible flux decline based on the efficiency of the chemical cleaning used

in this study. 100-FR-IR corresponds to the reversible flux decline caused by reversible adsorption. FR-RF corresponds to the reversible flux decline caused by concentration polarization. In addition, 100-IR corresponds to the cleaning efficiency.

The rejection properties of membranes were estimated by equation,

$$\xi = \left(1 - \frac{C_p}{C_f}\right) \times 100 \quad (5)$$

where ξ is the rejection rate, C_p is the permeate concentration, and C_f is the feed concentration.

3. Results and discussion

3.1. Characteristics of the secondary petrochemical wastewater

For a better understanding of the fouling phenomenon occurring on membrane surfaces, a rigorous feed water analysis was carried out. As indicated in Table 1, the wastewater effluent shows the organic and brackish nature owing to the excellent UF removal of suspended solids. Chemical oxygen demand (COD) concentration (43 mg L^{-1}) suggests that the effluent contains organic compounds in great concentration which might be potential foulants on the subsequent RO membranes. UV_{254} , a good surrogate for aromaticity of the dissolved organic matter, suggests the great concentration of the aromatics. The turbidity is 0.21 ± 0.1 NTU which is lower than 1.0 NTU recommended

by the membrane manufacturer. Anion and cation ions include Na^+ , K^+ , Ca^{2+} , Mg^{2+} , Cl^- , NO_3^- , F^- , PO_4^{3-} , and SO_4^{2-} . The amounts of the more abundant ions are Ca^{2+} (38.84 mg L^{-1}), Na^+ (220.83 mg L^{-1}), Cl^- (266.83 mg L^{-1}), and SO_4^{2-} (336.60 mg L^{-1}). The inorganic compounds foul membrane in two possible growth tracks, surface crystallization and crystal deposition [7]. In addition, the organic fouling of RO membrane can be enhanced by multivalent cations, such as Ca^{2+} , Mg^{2+} , and Fe^{3+} [19,20].

Membrane fouling is mainly controlled by the electrostatic interactions between the organic compounds and the membrane surface (initial fouling) and among organic molecules (the development of fouling layer). The acidity of the wastewater effluent was determined by potentiometric titration and is shown in Fig. 1. The increase of the acidity from pH 3.0–8.0 is attributed to the deprotonation of the carboxylic functional groups, while the increase from pH 8.0–10.0 is attributed to the deprotonation of the phenolic functional groups. The increase from pH 3.0–5.0, as well as from pH 8.0–10.0, is more significant. It indicated that the petrochemical secondary effluent consists of a complex mixture of organic compounds with various charge characteristics. To further identify the primary constituents of the wastewater, the dissolved organic matter in the wastewater was characterized by GC-MS. The total GC chromatogram is shown in Fig. 2. The mass spectra were searched in NIST library. According to the characteristics of the petrochemical wastewater, aromatic compounds and hydrocarbon compounds were found to be the major chemicals. The more

Table 1
Quality of the petrochemical secondary effluent

Parameter	Average value
pH	7.30 ± 0.5
Turbidity (NTU)	0.21 ± 0.1
Conductivity ($\mu\text{S cm}^{-1}$)	970 ± 10
Hardness ($\text{mg CaCO}_3 \text{ L}^{-1}$)	212.17 ± 5.2
COD (mg L^{-1})	43 ± 3
$\text{UV}_{254 \text{ nm}}$ (ABS)	0.173 ± 0.02
Ca^{2+} (mg L^{-1})	38.84 ± 0.57
Na^+ (mg L^{-1})	220.83 ± 6.4
Mg^{2+} (mg L^{-1})	11.52 ± 1.05
Fe^{3+} (mg L^{-1})	4.76 ± 0.24
Cl^- (mg L^{-1})	266.83 ± 10.3
NO_3^- (mg L^{-1})	53.69 ± 3.4
SO_4^{2-} (mg L^{-1})	336.60 ± 15.2
F^- (mg L^{-1})	1.52 ± 0.02
B^- (mg L^{-1})	0.754 ± 0.09
PO_4^{3-} (mg L^{-1})	1.51 ± 0.12

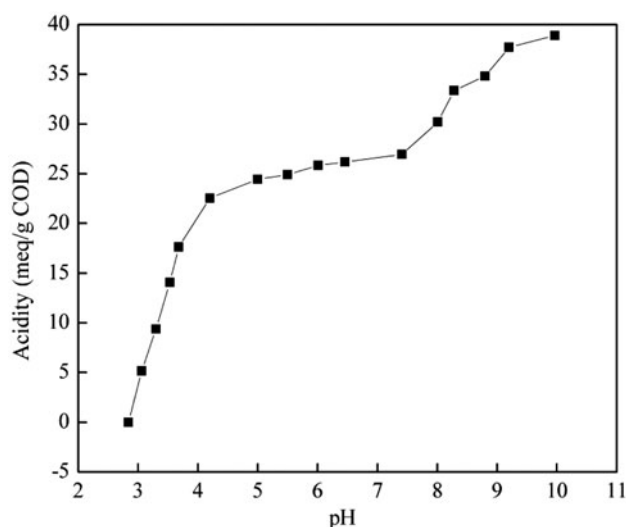


Fig. 1. Acidity of the petrochemical secondary wastewater as a function of pH.

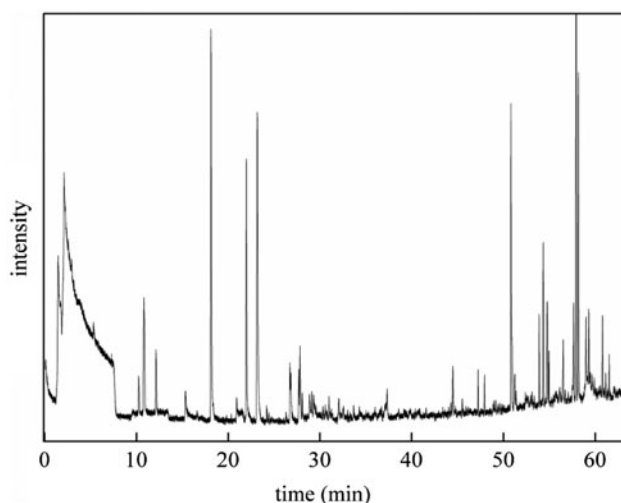


Fig. 2. The total GC chromatogram of the dissolved organic matter.

abundant organics were benzene (2.93 min, 1.03 wt%), dimethylbenzene (10.81 min, 6.26 wt%), phenol (18.13 min, 10.16 wt%), methylphenol (23.18 min, 16.85 wt%), xylene (27.82 min, 5.96 wt%), benzeneacetic acid (50.81 min, 8.25 wt%), n-octadecane (54.34 min, 2.91 wt%), dibutyl phthalate (57.92 min, 12.73 wt%), and n-hexadecanoic acid (59.00 min, 1.66 wt%). The mass fractions of all compounds are the relative amount. Both carboxylic functional groups and phenolic functional groups are present in the wastewater. The result is in accordance with the acidity of the wastewater. The aromatics have the hydrophobic structure, benzene ring, which is more prone to be adsorbed on the membrane surface than the hydrophilic organics. On the other hand, the fouling is also controlled by the electrostatic force between the charge group of the organics (carboxylic group and phenolic functional groups) and the charged membrane surface. If pH is less than 3.0, the organic compounds are fully protonated and behave as hydrophobic uncharged molecules. The charge properties of organic matters diminish through the neutralization of functional groups ($-\text{COOH}$, $-\text{OH}$). The organics are more easily adsorbed on the membrane surface because of the absence of electrostatic repulsion. At elevated pH (e.g. 10.0), the membrane surface is negatively charged and some organic compounds (e.g. benzeneacetic acid and methylphenol) are also negatively charged. The electrostatic repulsion between membrane surface and the organics increases due to the deprotonation of the carboxylic functional groups and phenolic functional groups of the organics. The increasing electrostatic repulsion inhibits the foulant from approaching the

membrane surface. As indicated by GC-MS results, both the phenolic functional groups and the carboxylic functional groups exist in the wastewater. Nevertheless, the carboxylic groups are the predominantly charged functional groups because the effluent is near neutral.

3.2. Flux behavior of the CPA2 membrane for tested wastewaters

Experiments with varying operating conditions were carried out to investigate whether or not concentration polarization or fouling contributed to flux decline. The standard experiment conditions were temperature $25.0 \pm 0.1^\circ\text{C}$, pH 7.0 ± 0.1 , TMP 20 ± 0.1 bar, and crossflow velocity $9.8 \times 10^{-2} \text{ms}^{-1}$. When the effect of the single factor on the flux decline was studied, the other factors were kept at constant.

The extent of irreversible fouling is strongly dependent on the efficiency of chemical cleaning. Hence, the cleaning efficiency of various agents was studied and the results are shown in Fig. 3. As described in Fig. 3, cleaning efficiency was 27.6% after the fouled membrane cleaned by DI water, which implied that the fouling layer on the membrane surface was largely irreversible. Conventional cleaning agents, such as NaOH (pH 11.0), 100 mM NaCl, 20 mM EDTA, HCl (pH 3.0), and 10 mM SDS, were used to remove the foulants on the membrane surface. Cleaning solutions were used at ambient pH except NaOH and HCl. Alkaline solution (NaOH, pH 11.0) exhibited the best cleaning performance in permeability recovery. It indicates the fact that the organic fouling is the dominant

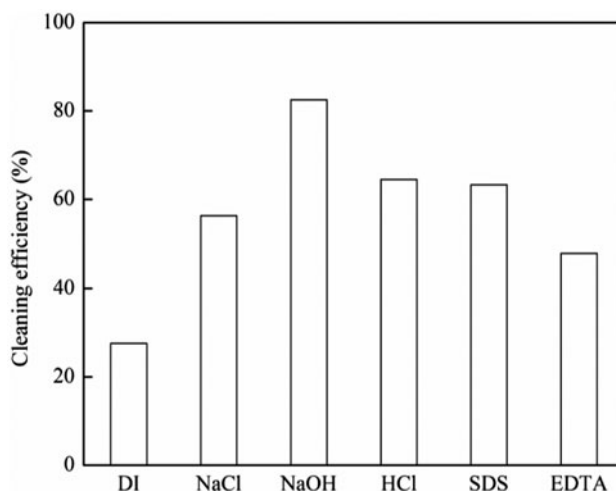


Fig. 3. Cleaning efficiencies of various cleaning solution. Conditions for fouling experiments were pH 7.0 ± 0.1 , temperature $25.0 \pm 0.1^\circ\text{C}$, TMP 20 ± 0.1 bar and crossflow velocity $9.8 \times 10^{-2} \text{ms}^{-1}$.

fouling mechanism during the reclamation of the effluent. In the case of NaOH cleaning, the organics adhered on the membrane surface are hydrolyzed at high pH levels. On the other hand, both the organics and membrane surface are charged more negatively, leading to strong electrostatic repulsion. A higher cleaning efficiency can be achieved by the combined agent or the dual-step cleaning [21]. The cleaning efficiency of NaOH solution (82.3%) was very much higher than that of the DI water's (25.4%). Considering the cleaning efficiency and the economy, we still selected the NaOH solution (pH 11.0) as the optimal cleaning agent. Hence, the extent of irreversible fouling was determined based on the efficiency of NaOH cleaning. The flux decline caused by concentration polarization, reversible and irreversible fouling is compared in Table 2.

An interesting finding from Table 2 is that a similar trend was obtained at various pHs. The flux decline due to concentration polarization was almost the same. The contents in the concentration polarization boundary layer are mainly inorganic salt and the organic compounds. The concentration polarization is more dependent on the soluble salt concentration than the organics' charge characteristics. For all the conditions, flux decline due to fouling is greater than that due to concentration polarization. Similar results had been obtained by Kaya et al. [13]. The organics deposited onto the membrane surface, leading to membrane fouling. Flux decline due to reversible fouling was the greatest among all the three causes. The reversible flux decline was much greater than the irreversible one. For example, the reversible flux decline was about four times than the irreversible one at pH 10.0. The fact indicates that the fouling is mainly due to "reversible" one, which is caused by concentration polariza-

tion and reversible fouling. It can be controlled through optimizing the operating conditions and a proper membrane cleaning. However, in some sense, what is more interesting is the study of irreversible fouling, which remains after long-term cycles of running-backflushing-cleaning procedures.

3.3. Effect of fouling on rejection

Rejection efficiencies were determined based on Cl^- measurements. The rejection of salt increased within 100 min (Fig. 4). The subsequent increase in salt rejection was marginal compared to the initial improvement. The phenomenon suggests that the initial foulant deposition onto the membrane surface is much more effective for enhancing salt rejection. Initial increase might be due to the quick adsorption of foulants onto the membrane surface, which enhanced the resistant of the salt passage. Subsequent improvement might be due to the formation of an organic cake layer, which developed more slowly and was less effective in increasing salt rejection. This is consistent with the previous observation [22]. Improved salt rejection can be explained by Donnan exclusion [23], where Cl^- anions are repelled by negatively charged functional groups of the organics ($-\text{COOH}$). Counter Na^+ ions are retained to maintain solution neutrality. When the membrane is fouled by the effluent with pH 3.0, the initial rejection of salt is just 66.53%. It might be explained by significant flux decline due to immediate adsorption of the neutral molecules onto the membrane surface. The flux dropped significantly leading to an increase in salt concentration of permeate. However, the rejection of salt increased from 66.53 to 98.26% with the fouling development.

Table 2

The flux decline results and initial fouling rate of the CPA2 membrane at various operating conditions

Model		Initial fouling rate ($\Delta J/\Delta t$) $\mu\text{m s}^{-2}$	Total 100-RF	Concentration polarization FR-RF	Reversible fouling 100-FR-IR	Irreversible fouling IR
pH	3.0	0.094 ± 0.003	46.9 ± 3.4	10.3 ± 0.6	20.4 ± 1.3	16.1 ± 2.5
	7.0	0.074 ± 0.003	36.1 ± 1.2	10.3 ± 0.8	18.2 ± 0.9	7.6 ± 0.9
	10	0.068 ± 0.004	34.7 ± 1.2	10.4 ± 0.5	17.1 ± 0.6	7.1 ± 0.3
T °C	15	0.061 ± 0.001	44.3 ± 2.7	11.9 ± 0.2	20.4 ± 0.8	11.9 ± 1.1
	25	0.074 ± 0.003	36.1 ± 1.2	10.3 ± 0.8	18.2 ± 0.9	7.6 ± 0.9
	35	0.174 ± 0.014	25.7 ± 1.1	8.9 ± 0.9	11.9 ± 0.6	4.9 ± 0.3
P bar	10	0.048 ± 0.010	32.9 ± 1.6	8.8 ± 0.4	19.3 ± 0.5	4.8 ± 0.7
	20	0.074 ± 0.003	36.1 ± 1.2	10.3 ± 0.8	18.2 ± 0.9	7.6 ± 0.9
	30	0.088 ± 0.003	42.5 ± 2.5	15.4 ± 0.3	14.6 ± 1.3	12.4 ± 0.3
U m s^{-1}	9.8×10^{-2}	0.074 ± 0.003	36.1 ± 1.2	10.3 ± 0.8	18.2 ± 0.9	7.6 ± 0.9
	20×10^{-2}	0.070 ± 0.003	32.2 ± 1.3	9.1 ± 0.5	16.9 ± 0.4	6.2 ± 0.7
	30×10^{-2}	0.068 ± 0.004	24.5 ± 1.6	7.5 ± 0.4	12.1 ± 0.8	4.9 ± 0.3

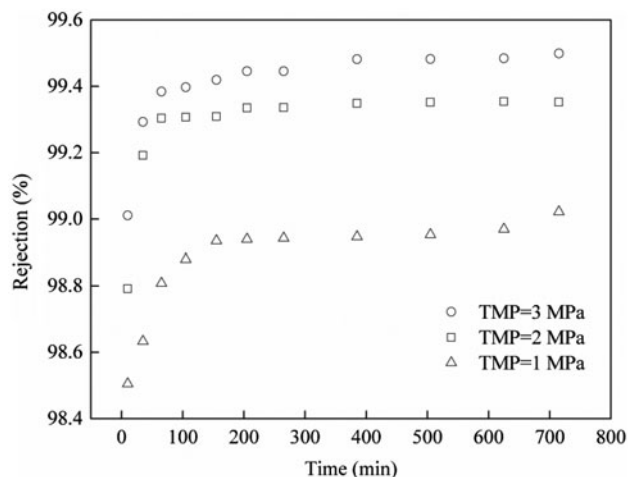


Fig. 4. Temporal evolution of salt rejection.

3.4. Fouling layer characteristics

3.4.1. Organic composition of fouling layer

To ascertain the nature of the fouling layer, organic contents of the fouling layer on a dry membrane and the physically stripped fouling layer were characterized and shown in Fig. 5. The physically stripped fouling layer was obtained after fouling-cleaning experiment. The fouling layer bound tightly to the membrane could hardly be physically stripped at the end of the experiment.

As shown in Fig. 5(a), the virgin membrane shows the typical pattern of the aromatic polyamide composite membrane with polysulfone support layer [24]. As foulants got deposited onto the coating layer of the membranes, the absorbance spectrum of the underlying polyamide composite membrane became less

apparent, especially the peaks around 1,240, 1,290, and 1,320 cm^{-1} (aromatic amines I, II, and III stretching, respectively), 1,480 and 1,580 cm^{-1} (polysulfonyl group) and 700–900 cm^{-1} (aromatics bond bending). However, the amide peaks (1,540 and 1,660 cm^{-1}) increased in absorbance intensity significantly. In addition, the amide peak of the virgin membrane at 1,660 cm^{-1} was shifted to lower wave numbers (1,635 cm^{-1}) after rather long-time fouling. The shift could be attributed to the fact that some electronegative atoms in foulants are bonded to polyamide chains through amide II groups (N–H). The peak at 1,050 cm^{-1} in the IR spectrum of fouled membrane is assigned to the silicon oxide bond of clay minerals [25]. After cleaning, the spectrum profiles were similar to that of the virgin membrane's. These results provide strong evidence that organic compounds are readily adsorbed onto the membrane surface, and the foulants can be partially removed by the chemical cleaning.

From Fig. 5(a), it can be seen that only partial foulants on the membrane surface can be removed by aggressive chemical cleaning. The residuary foulants was directly related to irreversible fouling. Hence, foulants were stripped off the cleaned membrane and analyzed by FTIR. The result is shown in Fig. 5(b). Bending of C–H at 670, 720, and 870 cm^{-1} and stretching of C=C near 1,425 cm^{-1} suggest the presence of the aromatics [26]. The minor peak at 1,135 cm^{-1} is assigned to polysaccharide-like material [27]. The minor peaks at 1,640 and 1,725 cm^{-1} are assigned to C=O stretch for amide and ester, respectively. The result is quite well accorded to the phenomenon that amide peaks increased in absorbance intensity, observed in Fig. 5(a). The small peak at 2,925 cm^{-1} is assigned to C–H stretch for alkanes [28]. The minor

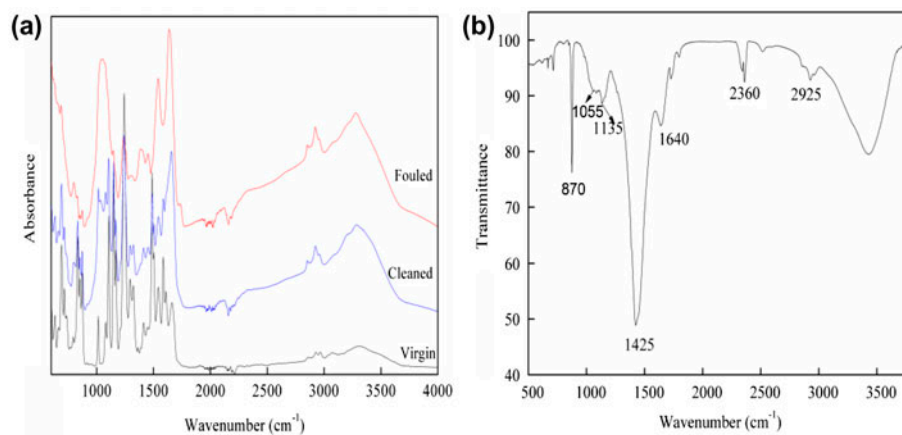


Fig. 5. FTIR spectra of (a) virgin, cleaned and fouled membranes and (b) physically stripped fouling layer.

peak at $1,055\text{ cm}^{-1}$ is assigned to the silicon oxide bond of clay minerals which is also observed in Fig. 5(a). The double peaks at $2,340$ and $2,360\text{ cm}^{-1}$ are assigned to the adsorption of CO_2 [29]. The above results provide evidence that the dominant organic foulants were found to be the aromatics. Combining

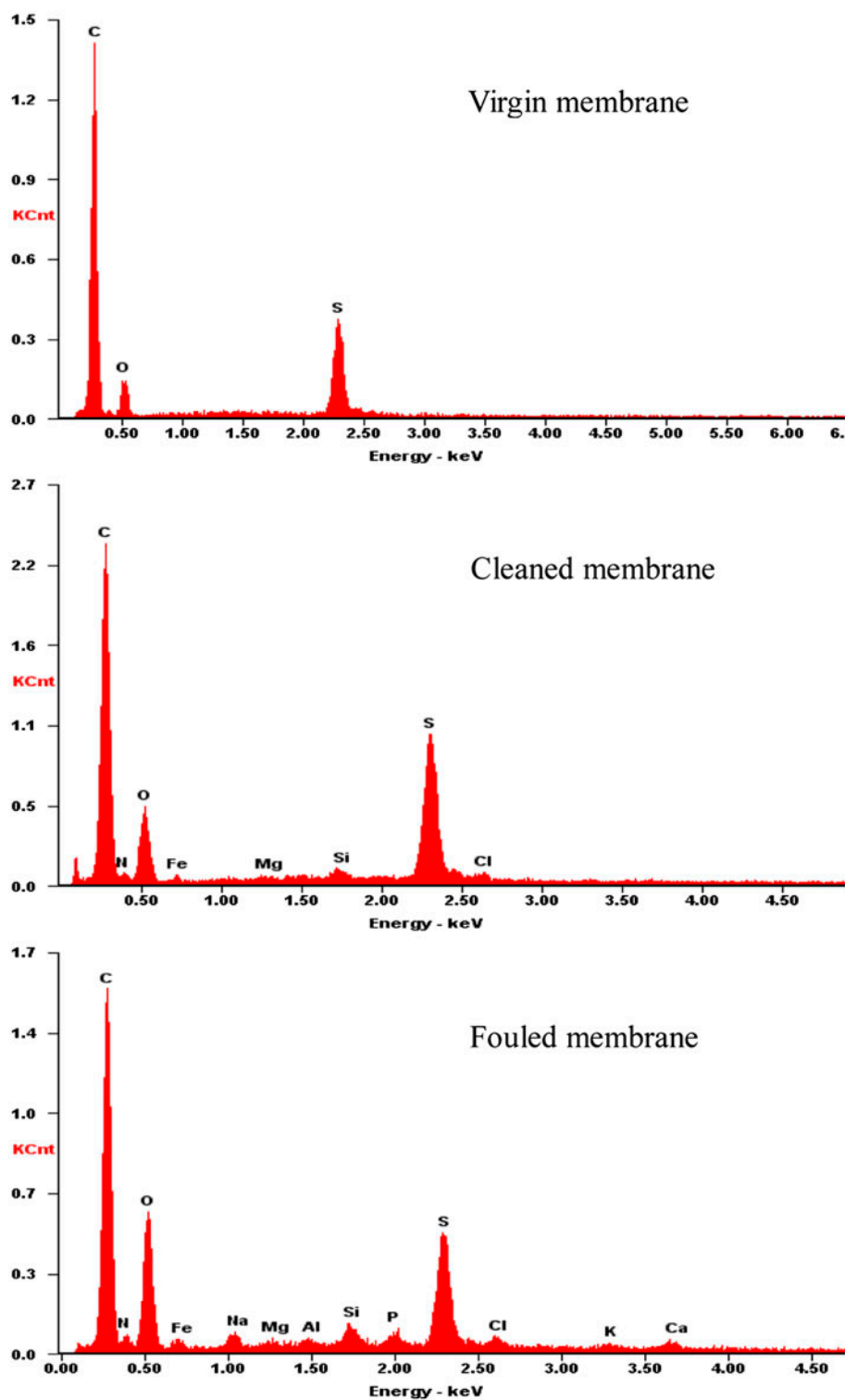


Fig. 6. EDS images of membranes.

with the results of GC-MS, we found that the aromatics are likely to be phenol, methylphenol, benzeneacetic acid, dibutyl phthalate, and xylenol.

3.4.2. Inorganic composition of fouling layer

The elemental composition of the virgin, cleaned, and fouled membranes obtained by EDX analyses was shown in Fig. 6. The virgin membrane only exhibited the presence of three major elements (C, O, and S). On the fouled membrane, a significant increase in the atom ratio of oxygen was observed which is attributable to accumulation of the organic compounds. Small quantities of metal such as Fe, Mg, Si, Al, and Ca were also detected, which were probably multi-valent cations complexed with organic molecules entering the cake layer [30]. Among various inorganic elements, Fe, P, Na, and Cl were found to be prominent constituents of the foulants, indicating that the compositions of the inorganic foulants were closely associated with the feed water qualities. After membrane cleaning using NaOH solution (pH 11.0), most of the total amount of inorganic species were removed. EDX peaks for Na, Al, Ca, and P disappeared and EDX peaks for Fe, Mg, and Si decreased sharply. However, this removal was not associated with a complete FR. The observation suggested that irreversible fouling was most likely caused by the residual organic foulants.

3.5. Mechanism involved in the evolution of irreversible fouling during the reclamation

As discussed above, irreversible fouling is most likely caused by the residual organic foulants and the aromatics are the dominant components of foulants. It is consistent with the fact that alkaline reagent (NaOH) is more effective in restoring the membrane permeability than the other reagents used. The metal cations, such as Fe^{3+} and Mg^{2+} , contribute to irreversible fouling to some extent. Similar results had been obtained by Kimura et al. for a pilot plant UF [31].

The organic compounds contained in the wastewater are not uniformly adsorbed onto the membrane surface [32,33]. Some fractions of the organic matters are preferentially adsorbed on or bound with the membrane. The aromatics have the hydrophobic structure, benzene ring, which is more prone to be adsorbed on the membrane surface through the hydrophobic force. The fouling is also determined by the electrostatic interaction [14]. The repulsion force between the negatively charged functional groups

(-COOH) and the negatively charged membrane surface leads to the reduction in fouling (Table 2). While the attractive force between the positively charged functional groups (-NH₂) and the negatively charged membrane surface leads to the increase of the fouling. In addition, the hydrogen bond also plays an important role on the membrane fouling [34]. IR measurement has been the most often employed for testing the existence and the strength of hydrogen bond [35]. The stretching vibration of proton-donating bond is typically shifted to red upon hydrogen bond formation. This red shift is correlated with the strength of the hydrogen bond as well as with the bond length. In the section 3.4.1, the IR peak of amide was shifted to red, which indicated that the H-bond between the foulants and the membrane were formed after long fouling. Contreras et al. [36] studied adsorption of organic foulants on membrane surface by quartz-crystal microbalance with dissipation monitoring. The results showed that adsorption of protein on hydrophilic membrane surface was dominated by hydrogen bond formation and electrostatic attraction. When the feed contains a mixture of contaminants, membrane fouling is more severe due to the synergistic effect [37], such as hydrophobic force, electrostatic force, and hydrogen bond formation. Metal cations cause membrane fouling by enhancing the aggregation of organic molecules in solution [25] and/or by neutralizing the negative charge of the membrane surface [38].

4. Conclusions

Fouling behaviors of a RO membrane fed with UF-pretreated petrochemical secondary effluent were investigated. It has been found that membrane fouling in the case of the filtration of solution containing organic compounds was dominated by organic fouling. The flux decline due to fouling was found to dominate over concentration polarization. The salt rejection was improved upon fouling occurring due to Donnan exclusion by the organics adsorbed on the membrane surface. With the microanalysis of fouling layer characteristics after membrane cleaning, irreversible fouling was most likely caused by the residual organic foulants. The aromatics, including phenol, methylphenol, benzeneacetic acid, dibutyl phthalate, and xylenol were proposed to be the predominant organic foulants causing irreversible fouling. Metal cations, such as Fe^{3+} and Mg^{2+} , contributed to irreversible fouling to some extent. The fouling rate and extent of flux decline can be related to synergetic effects of hydrophobic force, electrostatic force, and hydrogen bond formation.

Acknowledgments

This work was supported by National Science and Technology Support Program (grant number 2012BA C02B03).

Nomenclature

J	—	permeation flux ($\text{mL m}^{-2} \text{min}^{-1}$)
t	—	permeation measuring time (min)
U	—	crossflow velocity (m s^{-1})
P	—	operation pressure (bar)
R	—	resistance (m^{-1})

Greek letters

μ	—	viscosity (N s m^{-2})
$\Delta\pi$	—	osmotic pressure (bar)

Subscript/superscript

b	—	wastewater
0	—	initial state
w	—	pure water
fw	—	pure water through fouled membrane
cw	—	pure water through cleaned membrane
m	—	membrane
l	—	fouling layer
f	—	feed solution
p	—	permeate solution

References

- [1] C.W. Lee, S.D. Bae, S.W. Han, L.S. Kang, Application of ultrafiltration hybrid membrane processes for reuse of secondary effluent, *Desalination* 202 (2007) 239–246.
- [2] Z. Steiner, J. Miao, R. Kasher, Development of an oligoamide coating as a surface mimetic for aromatic polyamide films used in reverse osmosis membranes, *Chem. Commun.* 47 (2011) 2384–2386.
- [3] M.A. Shannon, P.W. Bohn, M. Elimelech, J.G. Georgiadis, B.J. Mariñas, A.M. Mayes, Science and technology for water purification in the coming decades, *Nature* 452 (2008) 301–310.
- [4] L. Braeken, B. Van der Bruggen, C. Vandecasteele, Flux decline in nanofiltration due to adsorption of dissolved organic compounds: Model prediction of time dependency, *J. Phys. Chem. B* 110 (2006) 2957–2962.
- [5] R.P. Schneider, L.M. Ferreira, P. Binder, J.R. Ramos, Analysis of foulant layer in all elements of an RO train, *J. Membr. Sci.* 261 (2005) 152–162.
- [6] D. Rana, T. Matsuura, Surface modifications for anti-fouling membranes, *Chem. Rev.* 110 (2010) 2448–2471.
- [7] J. Luo, L. Ding, Y. Wan, P. Paullier, M.Y. Jaffrin, Fouling behavior of dairy wastewater treatment by nanofiltration under shear-enhanced extreme hydraulic conditions, *Sep. Purif. Technol.* 88 (2012) 79–86.
- [8] S.S. Sablani, M.F.A. Goosen, R. Al-Belushi, M. Wilf, Concentration polarization in ultrafiltration and reverse osmosis: A critical review, *Desalination* 141 (2001) 269–289.
- [9] W. Guo, H.H. Ngo, J. Li, A mini-review on membrane fouling, *Bioresour. Technol.* 122 (2012) 27–34.
- [10] S.S. Madaeni, M.R. Eslamifard, Recycle unit wastewater treatment in petrochemical complex using reverse osmosis process, *J. Hazard. Mater.* 174 (2010) 404–409.
- [11] C. Benito-Alcázar, M.C. Vincent-Vela, J.M. Gozálviz-Zafrilla, J. Lora-García, Study of different pretreatments for reverse osmosis reclamation of a petrochemical secondary effluent, *J. Hazard. Mater.* 178 (2010) 883–889.
- [12] J.J. Qin, M.N. Wai, M.H. Oo, K.A. Kekre, H. Seah, Feasibility study for reclamation of a secondary treated sewage effluent mainly from industrial sources using a dual membrane process, *Sep. Purif. Technol.* 50 (2006) 380–387.
- [13] Y. Kaya, H. Barlas, S. Arayici, Evaluation of fouling mechanisms in the nanofiltration of solutions with high anionic and nonionic surfactant contents using a resistance-in-series model, *J. Membr. Sci.* 367 (2011) 45–54.
- [14] H. Li, Y. Lin, Y. Luo, P. Yu, L. Hou, Relating organic fouling of reverse osmosis membranes to adsorption during the reclamation of secondary effluents containing methylene blue and rhodamine B, *J. Hazard. Mater.* 192 (2011) 490–499.
- [15] W.S. Ang, M. Elimelech, Fatty acid fouling of reverse osmosis membranes: Implications for wastewater reclamation, *Water Res.* 42 (2008) 4393–4403.
- [16] S. Lee, M. Elimelech, Relating organic fouling of reverse osmosis membranes to intermolecular adhesion forces, *Environ. Sci. Technol.* 40 (2006) 980–987.
- [17] J.H. Tay, J. Liu, D.D. Sun, Effect of solution physicochemistry on the charge property of nanofiltration membranes, *Water Res.* 36 (2002) 585–598.
- [18] H. Li, Y. Lin, P. Yu, Y. Luo, L. Hou, FTIR study of fatty acid fouling of reverse osmosis membranes: Effects of pH, ionic strength, calcium, magnesium and temperature, *Sep. Purif. Technol.* 77 (2011) 171–178.
- [19] P. van den Brink, A. Zwijnenburg, G. Smith, H. Temmink, M. van Loosdrecht, Effect of free calcium concentration and ionic strength on alginate fouling in cross-flow membrane filtration, *J. Membr. Sci.* 345 (2009) 207–216.
- [20] H. Mo, K.G. Tay, H.Y. Ng, Fouling of reverse osmosis membrane by protein (BSA): Effects of pH, calcium, magnesium, ionic strength and temperature, *J. Membr. Sci.* 315 (2008) 28–35.
- [21] W.S. Ang, N.Y. Yip, A. Tiraferri, M. Elimelech, Chemical cleaning of RO membranes fouled by wastewater effluent: Achieving higher efficiency with dual-step cleaning, *J. Membr. Sci.* 382 (2011) 100–106.
- [22] C.Y. Tang, Y.N. Kwon, J.O. Leckie, Characterization of humic acid fouled reverse osmosis and nanofiltration membranes by transmission electron microscopy and streaming potential measurements, *Environ. Sci. Technol.* 41 (2006) 942–949.
- [23] C.Y. Tang, Y.N. Kwon, J.O. Leckie, Fouling of reverse osmosis and nanofiltration membranes by humic acid—Effects of solution composition and hydrodynamic conditions, *J. Membr. Sci.* 290 (2007) 86–94.
- [24] W. Lee, C.H. Ahn, S. Hong, S. Kim, S. Lee, Y. Baek, J. Yoon, Evaluation of surface properties of reverse osmosis membranes on the initial biofouling stages under no filtration condition, *J. Membr. Sci.* 351 (2010) 112–122.

- [25] W.Y. Ahn, A.G. Kalinichev, M.M. Clark, Effects of background cations on the fouling of polyethersulfone membranes by natural organic matter: Experimental and molecular modeling study, *J. Membr. Sci.* 309 (2008) 128–140.
- [26] H.J. Jeong, M.A. Kakimoto, Y. Imai, Synthesis and characterization of novel polyarylates from 2,5-bis(4-hydroxyphenyl)-3,4-diphenylpyrrole and various aromatic dicarboxylic acids, *J. Polym. Sci., Part A: Polym. Chem.* 32 (1994) 1057–1062.
- [27] C. Jarusutthirak, G. Amy, J.P. Croué, Fouling characteristics of wastewater effluent organic matter (EfOM) isolates on NF and UF membranes, *Desalination* 145 (2002) 247–255.
- [28] R.A. MacPhail, H.L. Strauss, R.G. Snyder, C.A. Elliger, Carbon-hydrogen stretching modes and the structure of n-alkyl chains. 2. Long, all-trans chains, *J. Phys. Chem.* 88 (1984) 334–341.
- [29] F. Fleyfel, J.P. Devlin, Carbon dioxide clathrate hydrate epitaxial growth: Spectroscopic evidence for formation of the simple type-II carbon dioxide hydrate, *J. Phys. Chem.* 95 (1991) 3811–3815.
- [30] Y. Zhao, L. Song, S.L. Ong, Fouling behavior and foulant characteristics of reverse osmosis membranes for treated secondary effluent reclamation, *J. Membr. Sci.* 349 (2010) 65–74.
- [31] K. Kimura, Y. Hane, Y. Watanabe, G. Amy, N. Ohkuma, Irreversible membrane fouling during ultrafiltration of surface water, *Water Res.* 38 (2004) 3431–3441.
- [32] B. Van der Bruggen, L. Braeken, C. Vandecasteele, Flux decline in nanofiltration due to adsorption of organic compounds, *Sep. Purif. Technol.* 29 (2002) 23–31.
- [33] B. Van der Bruggen, L. Braeken, C. Vandecasteele, Evaluation of parameters describing flux decline in nanofiltration of aqueous solutions containing organic compounds, *Desalination* 147 (2002) 281–288.
- [34] A. Sotto, J.M. Arsuaga, B. Van der Bruggen, Sorption of phenolic compounds on NF/RO membrane surfaces: Influence on membrane performance, *Desalination* 309 (2013) 64–73.
- [35] S.J. Grabowski, Ab initio calculations on conventional and unconventional hydrogen bonds—Study of the hydrogen bond strength, *J. Phys. Chem. A* 105 (2001) 10739–10746.
- [36] A.E. Contreras, Z. Steiner, J. Miao, R. Kasher, Q. Li, Studying the role of common membrane surface functionalities on adsorption and cleaning of organic foulants using QCM-D, *Environ. Sci. Technol.* 45 (2011) 6309–6315.
- [37] Q. Li, Z. Xu, I. Pinnau, Fouling of reverse osmosis membranes by biopolymers in wastewater secondary effluent: Role of membrane surface properties and initial permeate flux, *J. Membr. Sci.* 290 (2007) 173–181.
- [38] G. Amy, J. Cho, Interactions between natural organic matter (NOM) and membranes: Rejection and fouling, *Water Sci. Technol.* 40 (1999) 131–139.